Elsevier Editorial System(tm) for Fuel
Manuscript Draft

Manuscript Number:

Title: Growth Characteristics of Polycyclic Aromatic Hydrocarbons in Dimethyl Ether Diffusion Flame

Article Type: Original Research Paper

Keywords: Dimethyl ether; Diffusion flame; Polycyclic aromatic hydrocarbons; Soot; Laser-induced fluorescence; Laser-induced incandescence

Corresponding Author: Dr. Kazuhiro Hayashida, Ph.D

Corresponding Author's Institution: Kitami Institute of Technology

First Author: Kazuhiro Hayashida, Ph.D

Order of Authors: Kazuhiro Hayashida, Ph.D; Toshio Mogi; Kenji Amagai; Masataka Arai

Abstract: The growth characteristics of polycyclic aromatic hydrocarbons (PAHs) in laminar dimethyl ether (DME) diffusion flame were investigated experimentally. Methane and propane laminar diffusion flames were also investigated for a comparison of their combustion characteristics. Laser-induced fluorescence (LIF) and laser-induced incandescence (LII) techniques were used to measure the relative concentration of soot and PAHs, respectively. Two-dimensional images of the OH-LIF, PAHs-LIF, and LII from soot were measured in the test flames. Furthermore, to investigate the growth characteristics of the PAHs in the flames, the fluorescence spectra of the PAHs were measured at several heights in the flames, using a spectrograph. The molecular size of the PAHs was estimated based on an emission wavelength region of the PAHs-LIF that varied along with the PAH size. The results show that although the PAHs were widely distributed within the unburned region similar to that of the methane and propane flames, the intensity and detection region of LII were much smaller than that of the methane and propane flames. The PAHs-LIF spectra indicated that the growth of the PAHs within the DME flame was much slower than the methane and propane flames, and thus a large number of small PAHs were discharged into the OH region distributed around the outer edge of the flame.

Suggested Reviewers: Eui Lee
Fire and Engineering Service Research, Korea Institute of Construction Technology
ejlee@kict.re.kr

Charles McEnally
Chemical Engineering and Center for Combustion Studies, Yale University
charles.mcenally@yale.edu

D. Mishra
Aerospace Engineering, Indian Institute of Technology
mishra@iitk.ac.in

Cover Letter

June 29, 2010

Dear Editor:

I would like to contribute our paper entitled "Growth Characteristics of Polycyclic Aromatic Hydrocarbons in Dimethyl Ether Diffusion Flame" for the Fuel, which is the high quality journal in the science and technology of fuel and energy.

Will you please consider our manuscript for publication? Thank you.

Yours sincerely,

Kazuhiro Hayashida

Dept. of Mechanical Engineering
Kitami Institute of Technology
165 Koen-cho, Kitami,
Hokkaido 090-8507, JAPAN

E-mail: hayashka@mail.kitami-it.ac.jp

Title of the paper

Growth Characteristics of Polycyclic Aromatic Hydrocarbons in Dimethyl Ether Diffusion Flame

Authors and affiliations

Kazuhiro HAYASHIDA [a,*], Toshio MOGI [b], Kenji AMAGAI [c], Masataka ARAI [c]

[a] *Department of Mechanical Engineering, Kitami Institute of Technology*

165 Koen-cho, Kitami, Hokkaido 090-8507, Japan

[b] *Safety Management Office of Engineering, The University of Tokyo*

7-3-1 Hongo, Bunkyo-ku, Tokyo 113-8656, Japan

[c] *Department of Mechanical System Engineering, Gunma University*

1-5-1 Tenjin-cho, Kiryu, Gunma 376-8515, Japan

*** Corresponding author**

Kazuhiro HAYASHIDA

Department of Mechanical Engineering, Kitami Institute of Technology

165 Koen-cho, Kitami, Hokkaido 090-8507, Japan

Phone&Fax: +81-157-26-9206

e-mail: hayashka@mail.kitami-it.ac.jp

Abstract

The growth characteristics of polycyclic aromatic hydrocarbons (PAHs) in laminar dimethyl ether (DME) diffusion flame were investigated experimentally. Methane and propane laminar diffusion flames were also investigated for a comparison of their combustion characteristics. Laser-induced fluorescence (LIF) and laser-induced incandescence (LII) techniques were used to measure the relative concentration of soot and PAHs, respectively. Two-dimensional images of the OH-LIF, PAHs-LIF, and LII from soot were measured in the test flames. Furthermore, to investigate the growth characteristics of the PAHs in the flames, the fluorescence spectra of the PAHs were measured at several heights in the flames, using a spectrograph. The molecular size of the PAHs was estimated based on an emission wavelength region of the PAHs-LIF that varied along with the PAH size. The results show that although the PAHs were widely distributed within the unburned region similar to that of the methane and propane flames, the intensity and detection region of LII were much smaller than that of the methane and propane flames. The PAHs-LIF spectra indicated that the growth of the PAHs within the DME flame was much slower than the methane and propane flames, and thus a large number of small PAHs were discharged into the OH region distributed around the outer edge of the flame.

Keywords: Dimethyl ether, Diffusion flame, Polycyclic aromatic hydrocarbons, Soot, Laser-induced fluorescence, Laser-induced incandescence

1. Introduction

Dimethyl ether (DME) has great potential to contribute to a sustainable society; it can produce syngas from various resources, such as biomass, animal waste, and sewage sludge as well as natural gas, liquid-fuel and coal. The physical properties of DME are similar to those of liquefied petroleum gas (LPG); the infrastructure of LPG can be utilized for the storage, handling, and distribution of DME [1]. In recent years, techniques that involved direct DME synthesis from syngas have been developed [2-4], and the techniques should reduce the cost of production of DME in large quantities. Therefore, DME is attractive as an alternative fuel for various combustion devices.

The application of DME in a compression-ignition (diesel) engine is especially suitable. Because DME exhibits a low boiling point (248 K) and a high cetane number (CN=55-60), a low auto-ignition temperature (623 K), fast mixture formation, prompt auto-ignition and excellent cold start can be achieved [5]. In addition, due to its high oxygen content (35% by weight) and lack of carbon-carbon bonds, a reduction in exhaust emissions, especially soot, has been confirmed [6-9]. Furthermore, the properties such as a high CN and a low evaporating temperature are useful for a homogeneous charge compression ignition (HCCI) engine. An investigation of an HCCI engine fueled with DME was performed [10,11], and mixtures of DME/hydrogen [12], DME/natural gas [13,14], and DME/methanol-reformed gas (MRG) [15] were applied to an HCCI engine for ignition timing control. DME can also be used in gas turbines and boilers as an LNG substitute. Lean-premixed combustion is an effective technology to reduce NO_x emission in continuous combustion systems, but spontaneous ignition or flashback can easily occur in the case of DME due to its low auto-ignition temperature and high burning velocity. To develop a combustion technology using DME with low NO_x for gas turbines and boilers, it is necessary to introduce a new concept and technology [16,17].

An understanding of the combustion properties of DME is important to optimize DME combustion in various combustion devices. A number of kinetic studies regarding the pyrolysis and oxidation of DME have been performed [18-24], and detailed chemical kinetic models of DME were recently developed by Fischer et al. [25] and Curran et al. [26]. Kaiser et al. [27] measured the profiles of chemical species in a DME-air premixed flat flame at atmospheric pressure and obtained profiles that were compared to computational results based on a kinetic model. They also presented a photograph of DME diffusion flame [27], and the photograph clearly showed the existence of luminosity from soot particles. However, no experimental data regarding the DME diffusion flame were reported in the article. The growth characteristics of the PAHs and subsequent soot formation mechanism in a DME diffusion

flame are not yet known.

In this study, we investigate the growth characteristics of polycyclic aromatic hydrocarbons (PAHs) in DME diffusion flame. The PAHs are considered to be precursors of soot particles from the molecular reactants in a flame. The PAHs are considered to be the building blocks that undergo chemical reactions to form incipient soot [28-30]. Laser-induced incandescence (LII) and laser-induced fluorescence (LIF) were applied to obtain information regarding soot and PAHs, respectively. We measured the two-dimensional distribution of the PAHs-LIF in a DME diffusion flame, and laser-induced incandescence (LII) was also measured to visualize the soot distribution. Furthermore, the growth characteristics of the PAHs were discussed based on the profiles of the PAHs-LIF spectra.

2. Experimental Apparatus and Method

The laser diagnostic system used in this study consisted of an excimer laser (Lambda Physic, LPX-150T), a spectrograph (Chromex, 250IS), and an ICCD camera (La-Vision, FlameStar II). Figure 1 shows schematics of the optical arrangements. For the two-dimensional measurements of the OH-LIF, PAHs-LIF, and LII from the soot (Fig. 1(a)), a narrow-band KrF excimer laser (linewidth: ~0.3 cm^{-1}, pulse duration: ~24 ns) was used for the excitation of the OH, PAHs, and soot particles. The wavelength of this laser could be tuned within a range of 247.8-248.8 nm. For the OH-LIF measurement, the wavelength of the laser was set to 248.457 nm to excite the $P_2(8)$ transition within the *A*-*X*(3,0) band of the OH molecule. The lower state population of the $P_2(8)$ transition was not sensitive to temperature variations in the vicinity of the flame front [31]. For the PAHs-LIF and LII measurements, because the excitation bands of the OH, hot-O_2, [31] and NO [32] existed in the tunable wavelength region of the KrF excimer laser, the wavelength of the laser was tuned to 248.469 nm, which did not coincide with the excitation lines of these molecules. The laser light was formed into a light sheet (0.5 mm×20 mm) by an aperture and was introduced into a target flame with a pulse energy of 100 mJ. Laser-induced emissions were detected by the ICCD camera, which was oriented perpendicular to the laser beam direction. The LIF and LII images were obtained by averaging 1000 laser shots.

Figure 1(b) shows the optical arrangement that was used for the emission spectra measurements. The laser light was focused with a spherical lens (*f*=1000 mm) and was introduced into the target flame. The laser-induced emissions were analyzed by the spectrograph with the ICCD camera, which had a resolution of 384 (horizontal)×288 (vertical) pixels. The grating of the spectrograph had 100 grooves/mm (blazed for 450 nm), and a

spectral bandpass of 300 nm could be captured with the ICCD camera. The spectrum within the 300 nm width was distributed over 384 rows in the ICCD camera, which resulted in a spectral resolution of 2.4 nm using an entrance slit width of 20 μm.

The test flame used in this study was a laminar jet DME diffusion flame at atmospheric pressure. In addition, methane and propane diffusion flames were used for a comparison of their combustion characteristics. The test burner consisted of two concentric nozzles with inner diameters of 6 mm and 56 mm. The fuels flowed through the inner nozzle, and the length of each flame was 30 mm. The flame length was defined as the distance from the nozzle to the luminous flame tip. The fuel flow rates were set to 0.11 L/min of DME, 0.08 L/min of methane and 0.05 L/min of propane. To stabilize the flames, an annular airflow (temperature: 298 K) was applied to the outer nozzle. The velocity of the laminar airflow was 0.5 m/s, which was measured by a thermal anemometer (Kanomax, Aneomaster model 24-6131). The flame temperature was measured using a Pt/Pt-Rh 13 % thermocouple with a bead diameter of 200 μm. The thermocouple was placed into the flame for a short period of time to minimize soot accumulation on the wires. The soot deposited on the thermocouple was burned off by a blue flame before each temperature measurement. The measured thermocouple temperatures were corrected to account for radiative heat losses, which assumed a spherical bead geometry. The correction was based on a procedure reported by Bradley et al. [33].

3. Results and Discussion

3.1. Planar distributions of soot, PAHs and OH

Figure 2 shows two-dimensional images of the LII, PAHs-LIF and OH-LIF obtained from the test flames. The acquisition procedures of these images were described in a previous study [34]. Photographs of the test flames are also shown in this figure. The luminosity of the DME diffusion flame was much weaker than that of the methane and propane flames, but the appearance of the luminous zone in the DME flame proves the existence of soot particles within the flame. A very low LII intensity from the DME flame implies a very low soot concentration, and the narrow detection region of the LII implies that the soot formation was relatively slower than the other flames. In contrast with the LII, the PAHs-LIF from the DME flame was widely distributed in the unburned region. Although the PAHs-LIF intensity of the DME flame was also lower than the methane and propane flames, a significant intensity difference (as with the LII) could not be confirmed. The OH-LIF images show that the OH radicals were

distributed around the outer edge of the flames, and a significant difference was not observed in the intensity. The LII and PAHs-LIF were detected within the OH-LIF region. In the OH-LIF images of the methane and propane flames, although it seems that some fluorescence was detected in the fuel region, this was due to an error in the data acquisition procedure [34].

3.2. Axial profiles of the temperature: LII, PAHs-LIF and OH-LIF

Figure 3 shows the axial temperature profiles of the test flames. The temperature of the DME flame within the fuel pyrolysis region was lower than the other flames. The flame temperatures just after the nozzle exit were 527 K (DME), 695 K (methane) and 744 K (propane), and each temperature increased sharply from the nozzle exit; the slope then changed slowly around z=16 mm (DME), 11 mm (methane), and 7 mm (propane), respectively. For all of the flames, the temperatures increased sharply again around z=23 mm and reached a peak around z=30 mm, which corresponds to the luminous flame tip region. The maximum temperature in the DME flame was 1888 K (z=31 mm), and this temperature was higher than the methane (1804 K at z=29 mm) and propane (1808 K at z=28 mm) flames.

Figures 4-6 show the relative intensity profiles of the LII, PAHs-LIF and OH-LIF on the flame axis along with the temperature profiles. The PAHs-LIF profiles suggest that aromatic rings quickly formed near the nozzle exit (z<5 mm) in each flame, and the concentrations of the PAHs subsequently increased along with the distance from the nozzle. Especially in the propane flame, the formation of an aromatic ring was relatively quick (z≈2 mm), and a rapid increase in the PAHs concentration was observed. The pyrolysis of propane generates propargyl (C_3H_3) radicals, and benzene (C_6H_6) and/or phenyl (C_6H_5) might be quickly formed by a propargyl recombination reaction [35]. Furthermore, because the species of an aromatic ring precursor were abundant compared to the methane flame [36], the rate of the PAHs was higher than that of the methane flame.

Regarding the DME flame, the rate of increase of the PAHs-LIF intensity was higher than that of the methane flame for the low-temperature region (z<15 mm). The concentration of acetylene (C_2H_2) and methyl radicals (CH_3) in a counterflow diffusion flame fueled by DME and methane was calculated by Yoon et al. [37]. Acetylene is known as the key species in the hydrogen abstraction and acetylene addition (HACA) mechanism [38], which is the one of the popular mechanisms for the growth of the PAHs under the pyrolytic condition. Their results indicated that the acetylene concentration in the DME flame is similar to that of the methane flame. In contrast, the concentration of methyl radical in the DME flame is much higher than the methane flame for a low-temperature condition (T<1500 K). Methyl radical is a building block for the synthesis of aromatic ring precursors such as propargyl

radical [39, 40]; therefore, the results of Figs. 4 and 5 reveal that the formation of an aromatic ring in the DME flame was quicker than the methane flame for the low-temperature condition.

In each flame, the peak value of the PAHs-LIF coincides with the location where the LII intensity quickly increases, and the PAHs-LIF intensity decreases with an increase in the LII intensity. Tosaka et al. [41] reported that large PAHs and soot particles were formed by condensation polymerization and dehydrogenation of 3-5 ring PAHs for temperatures in excess of 1400 K. This temperature corresponds to the appearance temperature of the LII in our flames, as shown in Figs. 4-6. The disappearance location of the PAHs-LIF coincides with the peak of the LII in the methane and propane flames. Meanwhile, because the disappearance location of the PAHs-LIF in the DME flame was almost the same as the LII, a large number of PAHs were oxidized by OH radicals before they transformed into soot particles. The LII and PAHs-LIF disappeared around the peak of the OH, which is the primary oxidant of soot.

3.3. Growth characteristics of the PAHs within the flames

The broadband excitation and emission characteristics of the PAH molecules complicate the spectroscopic analysis of PAHs in a flame. The selective excitation and detection of individual PAHs in a flame are difficult, such that a measurement of the concentration distribution of individual PAH has not been achieved by the LIF technique. Generally, because the energy separation between the electronic excited state and electronic ground state decreases with an increase in the size of the PAH, the fluorescence wavelength region shifts towards longer wavelengths as the size of the PAH increases [42]. Therefore, the growth characteristics from the PAHs to soot particles can be estimated from a PAHs-LIF spectrum obtained from a flame because the fluorescence detection wavelengths reflect the molecular size of the PAHs. Figure 7 shows the relationship between the peak wavelengths of the PAH-LIF and the carbon number of PAH. Benzene is also indicated in this figure. The data of peak wavelengths of each PAH-LIF were obtained from precious studies [43-45]. Individual PAHs in the vapor phase were excited by UV laser sources (excitation wavelength λ_{ex}=248 and 266 nm). Figure 7 clearly shows that the peak of the PAH-LIF shifts to longer wavelengths as the size of the PAH increases. For large PAHs (carbon number>24), fluorescence data for the vapor phase could not be found.

Figure 8 shows the emission spectra obtained from the test flames on the flame axis. From these figures, it was confirmed that the peak wavelength of emission shifts to longer wavelengths as it approaches the sooting regions. In these spectra, the peak observed at 496nm is the contribution from the second-order interference from the Mie

scattering at the excitation laser line (248 nm). The emission spectra obtained in the sooting region of z>26 mm of methane and z>18 mm of propane are considered to be LII because the PAHs-LIF was only slightly detected in these positions (see Figs. 5 and 6). The spectrum profiles near the sooting region in each flame were similar to that of the LII, whereas the profiles within the fuel pyrolysis region were different from one another. Variations in the spectral profile suggest that the small PAH grew to the large PAH as the sooting region was approached.

In the propane flame, the PAHs-LIF spectrum at z=2 mm had a peak around λ_{em}=360 nm, and this wavelength corresponds to the peak fluorescence wavelength of 2- or 3-ring aromatics. This result implies that benzene and/or phenyl were promptly formed by the propargyl recombination reaction as mentioned above, and the small PAHs such as naphthalene and phenanthrene were subsequently formed. At z=5 mm, fluorescence from the PAH molecules, which contain approximately 12 to 16 carbon atoms, primarily constituted the spectrum. In front of the sooting region (z=14 mm), the PAHs, which have over 20 carbon atoms, primarily constituted the spectrum. The molecular mass of the large PAHs (carbon number>20) was over 250 u, whereas the molecular mass of the soot nucleus was defined as 2000 u [46]. Thus, the results suggest that the soot nucleus can be easily formed by the polymerization and/or coagulation of large PAHs. The spectrum profile at z=17 mm is similar to the LII because this spectrum consists of the LII and LIF from large PAHs.

In the methane flame, PAHs-LIF was only slightly detected near the nozzle exit (z=2 mm). The PAHs-LIF appeared at z=5 mm, and the spectrum had a peak around 350nm. Although the benzene existed abundantly at this position, the contribution of benzene fluorescence to the observed spectrum should be small because benzene has a low quantum efficiency and a low molar absorptivity [47]. Therefore, the emission spectrum of z=5 mm primarily consisted of fluorescence from C_{10}~C_{13} aromatic components. Small variations of the spectrum profiles up to z=11 mm indicate that the growth of PAHs was relatively slow in this region. This is due to the low concentrations of both acetylene and methyl radicals in the low-temperature region of the methane diffusion flame [37]. In contrast, methyl radicals formed abundantly in the high-temperature region [37], such that the growth of the PAHs advanced rapidly around the high-temperature region (z>14 mm).

Regarding the DME flame, the fluorescence wavelength region shift towards longer wavelengths was not confirmed from z=5 mm to z=17 mm. This result implies that the growth of PAHs is very slow within the fuel pyrolysis region. Recently, the growth mechanism for the PAHs, methyl addition/cyclization (MAC), was proposed by Shukla et al. [48]. We determined that the growth of the PAHs in the DME flame was predominantly due to the

MAC mechanism, because the methyl radicals were abundant within the fuel pyrolysis region [37]. The MAC mechanism is not efficient for the growth of large PAHs due to a mass growth of only 14 u [48]. This characteristic explains the very slow growth of the PAHs in the DME flame. The contribution of the HACA mechanism must be small because the pyrolysis of DME generates only a small amount of acetylene under the low-temperature condition [37]. Hidaka et al. [49] reported that the pyrolysis of DME hardly yields a propyne (C_3H_4) and allene (AC_3H_4), which are important species in the aromatic ring formation and the PAH growth processes. Thus, the PAHs and subsequently formed soot concentrations in the DME flame were much lower than the methane and propane flames. Note that the spectrum of the DME flame at z=26 mm had a relatively high intensity in the short-wavelength region (λ_{em}<400 nm). This result proves a large number of small PAHs were discharged into the OH region along with a very slow growth characteristic of the PAHs.

4. Conclusions

The growth characteristics of PAHs in the DME diffusion flame were investigated by using laser diagnostic techniques. The main results are summarized as follows:

1. The PAHs-LIF from the DME flame is widely distributed within the unburned region similar to that of the methane and propane flames, whereas the LII detection region of the DME flame was much more narrow than that of the methane and propane flames. Furthermore, the LII intensity of the DME flame was much lower than the methane and propane flames.
2. The peak of the PAHs-LIF intensity coincides with the location where the LII intensity rapidly increases, and the PAHs-LIF intensity decreases with an increase in the LII intensity in each flame. The disappearance location of the PAHs-LIF in the DME flame was almost same as the LII, which is unlike the methane and propane flames whose disappearance location was the peak of the LII intensity.
3. The peak wavelength of the PAHs-LIF spectra shifts to longer wavelengths as the soot inception region was approached in each flame. The shift of the fluorescence wavelength region toward longer wavelengths suggested that the growth of the PAHs within the DME flame is much slower than that of the methane and propane flames.
4. A large number of small PAHs in the DME flame were discharged into the OH region and were oxidized by OH radicals.

Acknowledgements

The authors are grateful for permission to use the flash-photometry of Gunma University, Faculty of Engineering special equipment. This study was supported by KAKENHI, Gant-in-Aid for Young Scientists (B), 22760141, 2010.

References

[1] Semelsberger TA, Borup RL, Greene HL. Dimethyl ether (DME) as an alternative fuel. J Power Sources 2006;156:497-511.

[2] Ogawa T, Inoue N, Shikada T, Ohno Y. Direct Dimethyl Ether (DME) synthesis from natural gas. Stud Surf Sci Catal 2004;147:379-384.

[3] Ohno Y, Yagi H, Inoue N, Okuyama K, Aoki S. Slurry phase DME direct synthesis technology -100 tons/day demonstration plant operation and scale up study-. Stud Surf Sci Catal 2007;167:403-408.

[4] Li Y, Wang T, Yin X, Wu C, Ma L, Li H, Lv Y, Sun L. 100 t/a-Scale demonstration of direct dimethyl ether synthesis from corncob-derived syngas. Renewable Energy 2010;35:583-587.

[5] Arcoumanis C, Bae C, Crookes R, Kinoshita E. The potential of di-methyl ether (DME) as an alternative fuel for compression-ignition engines: A review. Fuel 2008;87:1014-1030.

[6] Fleisch T, McCarthy C, Basu A, Uldovich C, Charbonneau P, Slodowske W, Mikkelsen S-E, McCandless J. A new clean technology: demonstration of ULEV emissions on a Navistar diesel engine fueled with dimethyl ether. SAE Paper 950061; 1995.

[7] Sorenson SC, Mikkelsen S-E. Performance and emission of a 0.273 liter direct injection diesel engine fuelled with neat dimethyl ether. SAE Paper 950064; 1995.

[8] Kapus PE, Cartelleri WP. ULEV potential DI/TCI diesel passenger car engine operated on dimethyl ether. SAE Paper 952754; 1995.

[9] Maroteaux F, Descombes G, Jullien J. Investigation on exhaust emissions of a common rail high-speed direct injection diesel engine running with dimethyl ether. Int J Engine Research 2001;2:199-207.

[10] Sato S, Iida N. Analysis of DME homogeneous charge compression ignition combustion. SAE Paper 2003-01-1825; 2003.

[11] Ying W, Li H, Jie Z, Longbao Z. Study of HCCI-DI combustion and emissions in a DME engine. Fuel 2009;88:2255-2261.

[12] Narioka Y, Takagi Y, Yokoyama T, Iio S. HCCI combustion characteristics of hydrogen and hydrogen-rich natural gas reformate supported by DME supplement. SAE Paper 2006-01-0628; 2006.

[13] Chen Z, Konno M, Oguma M, Yanai T. Experimental study of CI natural gas/DME homogeneous charge engine. SAE Paper 2000-01-0329; 2000.

[14] Kong S-C. A study of natural gas/DME combustion in HCCI engines using CFD with detailed chemical kinetics. Fuel 2007;86:1483-1489.

[15] Shudo T, Takahashi T. Influence of reformed gas composition on HCCI combustion of onboard methanol-reformed gases. SAE Paper 2004-01-1908; 2004.

[16] Matsumoto R, Ozawa M, Ishihara I, Sasaki S, Takaichi M. Development of low-NOx DME multi-port burner. JSME International Journal Ser B 2006;49:245-252.

[17] Lee MC, Seo SB, Chung JH, Joo YJ, Ahn DH. Industrial gas turbine combustion performance test of DME to use as an alternative fuel for power generation. Fuel 2009;88:657-662.

[18] Benson SW. Pyrolysis of dimethyl ether. J Chem Phys 1956;25:27-31.

[19] Benson SW, Jain DVS. Further studies of the pyrolysis of dimethyl ether. J Chem Phys 1959;31:1008-1017.

[20] Anderson KH, Benson SW. Termination products and processes in the pyrolysis of dimethyl ether. J Chem Phys 1962;36:2320-2323.

[21] Held AM, Manthorne KC, Pacey PD, Reinholdt HP. Individual rate constants of methyl radical reactions in the pyrolysis of dimethyl ether. Can J Chem 1977;55:4128-4134.

[22] Batt L, Alvarado-Salinas G, Reid IAB, Robinson C, Smith DB. The pyrolysis of dimethyl ether and formaldehyde. Proc Combust Inst 1982;19:81-87.

[23] Dagaut P, Boettner J-C, Cathonnet M. Chemical kinetic study of dimethylether oxidation in a jet stirred reactor from 1 to 10 ATM: Experiments and kinetic modeling. Proc Combust Inst 1996;26:627-632.

[24] Dagaut P, Daly C, Simmie JM, Cathonnet M. The oxidation and ignition of dimethylether from low to high temperature (500–1600 K): Experiments and kinetic modeling. Proc Combust Inst 1998;27:361-369.

[25] Fischer SL, Dryer FL, Curran HJ. The reaction kinetics of dimethyl ether. I: High-temperature pyrolysis and oxidation in flow reactors. Int J Chem Kinet 2000;32:713-740.

[26] Curran HJ, Fischer SL, Dryer FL. The reaction kinetics of dimethyl ether. II: Low-temperature oxidation in flow reactors. Int J Chem Kinet 2000;32:741-759.

[27] Kaiser EW, Wallington TJ, Hurley MD, Platz J, Curran HJ, Pitz WJ, Westbrook CK. Experimental and Modeling Study of Premixed Atmospheric-Pressure Dimethyl Ether−Air Flames. J Phys Chem A 2000;104:8194-8206.

[28] Hepp H, Siegmann K, Sattler K. New aspects of growth mechanisms for polycyclic aromatic hydrocarbons in diffusion flames. Chem Phys Lett 1995;233:16-22.

[29] Vander Wal RL. Soot precursor material: visualization via simultaneous LIF-LII and characterization via TEM. Proc Combust Inst 1996;26:2269-2275.

[30] Richter H, Howard JB. Formation of polycyclic aromatic hydrocarbons and their growth to soot—a review of chemical reaction pathways. Progr Energy Combust Sci 2000;26:565-608.

[31] Andresen P, Bath A, Gröger W, Lülf HW, Meijer G, ter Meulen JJ. Laser-induced fluorescence with tunable excimer lasers as a possible method for instantaneous temperature field measurements at high pressures: checks with an atmospheric flame. Appl Opt 1988; 27:365-378.

[32] Schulz C, Yip B, Sick V, Wolfrum J. A laser-induced fluorescence scheme for imaging nitric oxide in engines. Chem Phys Lett 1995;242:259-264.

[33] Bradley D, Matthews KJ. Measurement of high gas temperatures with fine wire thermocouples. J Mech Eng Sci 1968;10:299-305.

[34] Hayashida K, Amagai K, Satoh K, Arai M. Experimental analysis of soot formation in sooting diffusion flame by laser-induced emissions. J Eng Gas Turbine Power, Trans ASME 2006;128:241-246.

[35] Miller JA, Melius CF. Kinetic and thermodynamic issue in the formation of aromatic compounds in flames of aliphatic fuels. Combust Flame 1992;91:21-39.

[36] McEnally CS, Pfefferle LD. Comparison of non-fuel hydrocarbon concentrations measured in coflowing nonpremixed flames fueled with small hydrocarbons. Combust Flame 1999;117:362-372.

[37] Yoon SS, Anh DH, Chung SH. Synergistic effect of mixing dimethyl ether with methane, ethane, propane, and ethylene fuels on polycyclic aromatic hydrocarbon and soot formation. Combust Flame 2008;154:368-377.

[38] Frenklach M, Clary DW, Gardiner WC, Stein SE. Detailed kinetic modeling of soot formation in shock-tube pyrolysis of acetylene. Proc Combust Inst 1985;20:887-901.

[39] Senkan S, Castaldi M. Formation of polycyclic aromatic hydrocarbons (PAH) in methane combustion: Comparative new results from premixed flames. Combust Flame 1996;107:141-150.

[40] McEnally CS, Prefferle LD. The effects of dimethyl ether and ethanol on benzene and soot formation in ethylene nonpremixed flames. Proc Combust Inst 2007;31:603-610.

[41] Tosaka S, Fujiwara Y, Murayama T. The effect of fuel properties on diesel engine exhaust particulate formation (The effect of molecular structure and carbon number). SAE paper 1989:No.891881.

[42] Berlman IB. Handbook of fluorescence spectra of aromatic molecules. New York: Academic Press; 1965.

[43] Satoh K, Hayashida K, Miyakawa T, Amagai K, Arai M. Laser measurement of polycyclic aromatic hydrocarbons (PAHs) (2nd report, Presumption of PAHs by laser-induced fluorescence spectrum). Transactions of the Japan Society of Mechanical Engineers Series B 2004;70:2183-2190.

[44] Ossler F, Metz T, Aldén M. Picosecond laser-induced fluorescence from gas-phase polycyclic aromatic hydrocarbons at elevated temperatures (I. Cell measurements). Appl Phys B 72 2001:465-478.

[45] Cignoli F, Zizak G, Benecchi S, Tencalla D. Atlas of fluorescence spectra of aromatic hydrocarbons (vol. 1). http://www.tempe.mi.cnr.it.

[46] Mckinnin JT, Howard JB. The roles of PAH and acetylene in soot nucleation and growth, Proc Combust Inst 1992; 24: 965-971.

[47] Beretta F, Cincotti V, D'alessio A, Menna P. Ultraviolet and visible fluorescence in the fuel pyrolysis regions of gaseous diffusion flames. Combust Flame 1985;61:211-218.

[48] Shukla B, Miyoshi A, Koshi M. Role of methyl radicals in the growth of PAHs. J Am Soc Mass Spectrom 2010;21:534-544.

[49] Hidaka Y, Sato K, Yamane M. High-temperature pyrolysis of dimethyl ether in shock waves. Combust Flame 2000;123:1-22.

Figure captions

Fig. 1

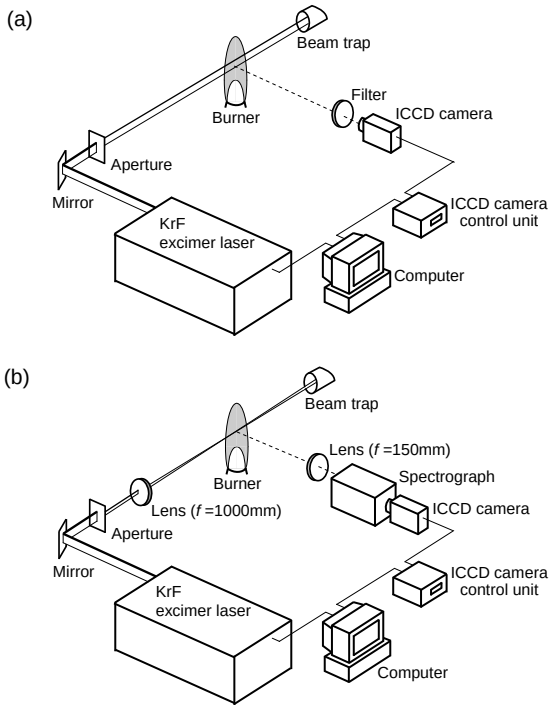
(a)
Beam trap
Filter
ICCD camera
Burner
Aperture
Mirror
ICCD camera
control unit
KrF
excimer laser
Computer
(b)
Beam trap
Lens (f =150mm)
Spectrograph
Burner
ICCD camera
Lens (f =1000mm)
Aperture
Mirror
ICCD camera
control unit
KrF
excimer laser
Computer

Fig. 2

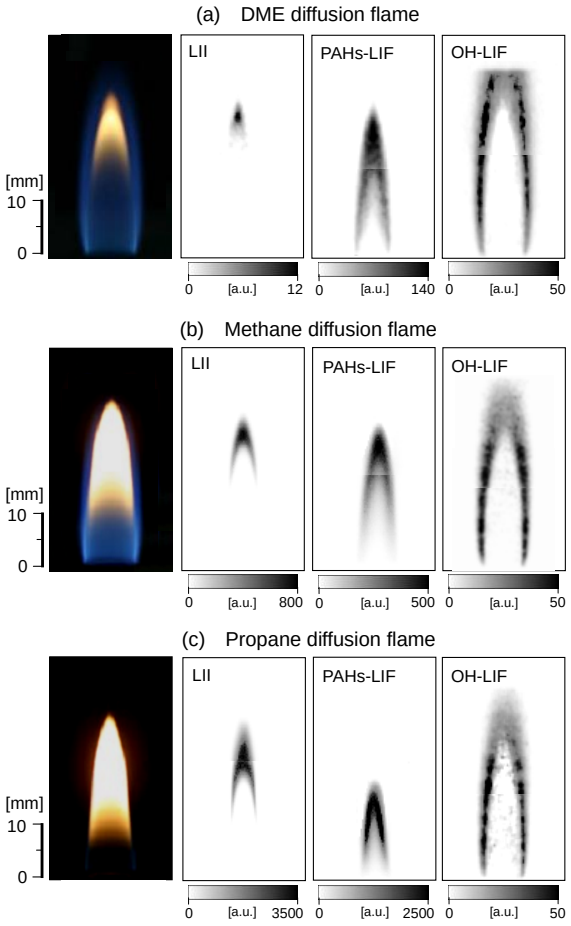
(a) DME diffusion flame
LII
PAHs-LIF
OH-LIF
[mm]
10
0
0 [a.u.] 12
0 [a.u.] 140
0 [a.u.] 50
(b) Methane diffusion flame
LII
PAHs-LIF
OH-LIF
[mm]
10
0
0 [a.u.] 800
0 [a.u.] 500
0 [a.u.] 50
(c) Propane diffusion flame
LII
PAHs-LIF
OH-LIF
[mm]
10
0
0 [a.u.] 3500
0 [a.u.] 2500
0 [a.u.] 50

Fig. 3

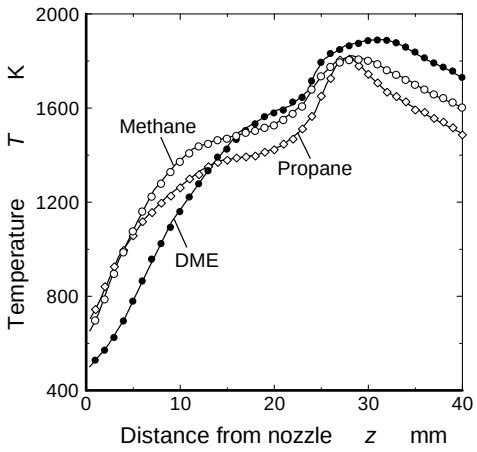
2000
1600
1200
800
400
Temperature T K
Methane
Propane
DME
0
10
20
30
40
Distance from nozzle z mm

Fig. 4

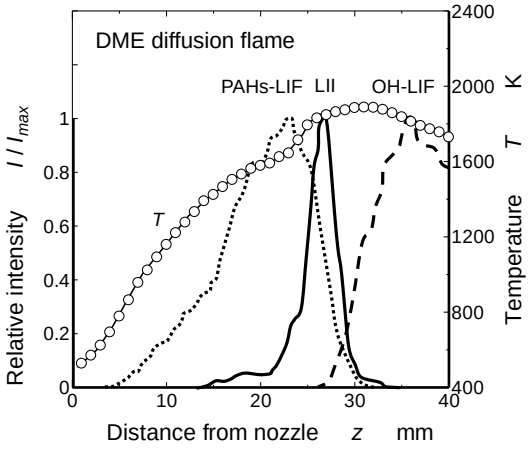
DME diffusion flame
PAHs-LIF
LII
OH-LIF
T
Relative intensity I / I_max
Temperature T K
Distance from nozzle z mm
0
0.2
0.4
0.6
0.8
1
400
800
1200
1600
2000
2400
0
10
20
30
40

Fig. 5

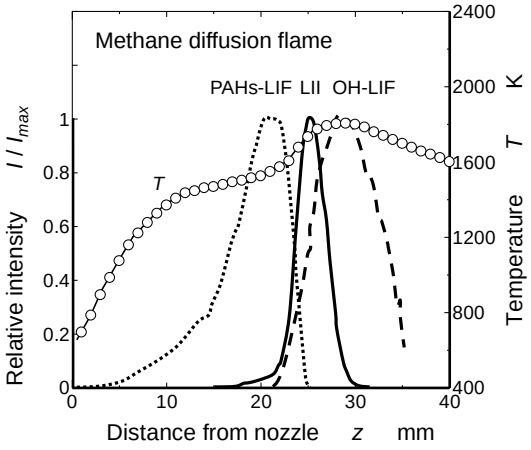
Methane diffusion flame
PAHs-LIF LII OH-LIF
T
Relative intensity I / I_max
Temperature T K
Distance from nozzle z mm
0
0.2
0.4
0.6
0.8
1
400
800
1200
1600
2000
2400
0
10
20
30
40

Fig. 6

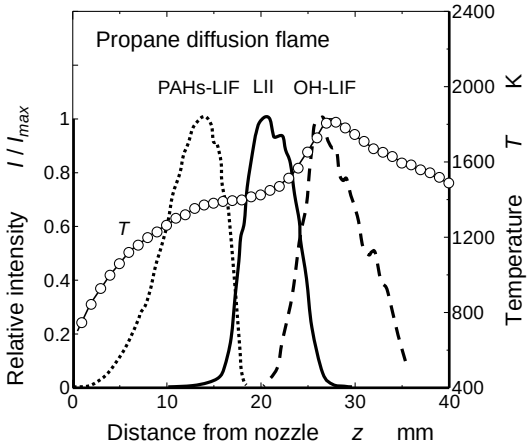
Propane diffusion flame
PAHs-LIF
LII
OH-LIF
T
Relative intensity I / I_max
Temperature T K
Distance from nozzle z mm
0
0.2
0.4
0.6
0.8
1
400
800
1200
1600
2000
2400
0
10
20
30
40

Fig. 7

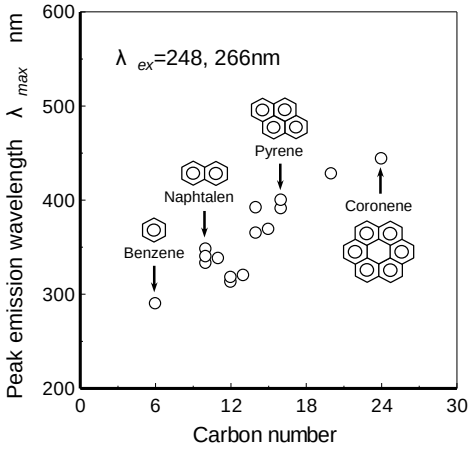
λ ex=248, 266nm
Peak emission wavelength λ max nm
Carbon number
Benzene
Naphtalen
Pyrene
Coronene
600
500
400
300
200
0
6
12
18
24
30

Fig. 8

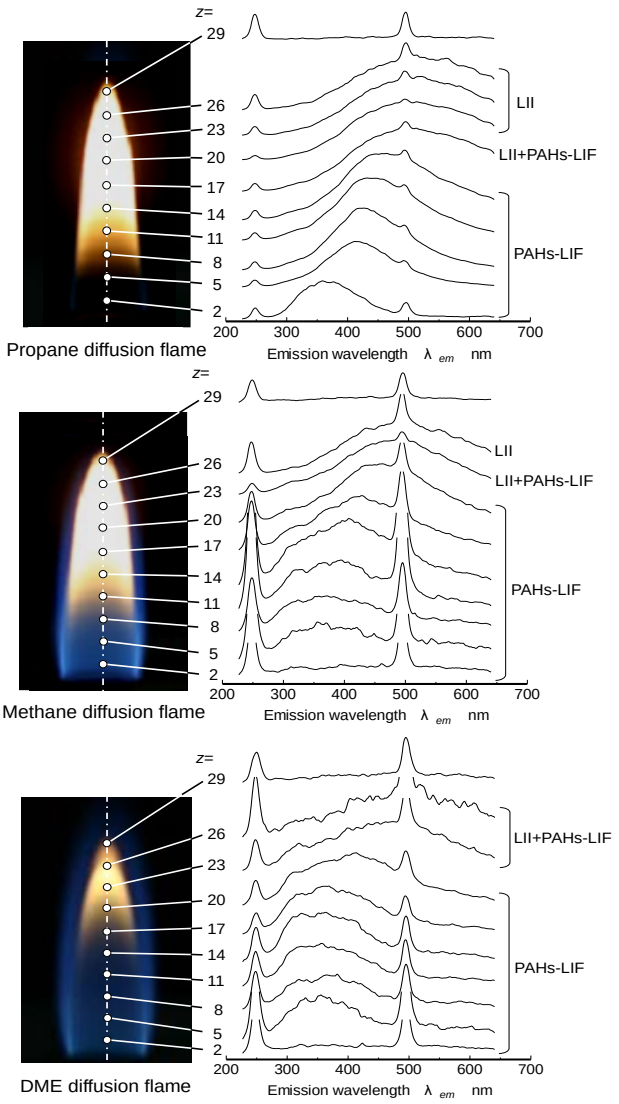
z=
29
26
23
20
17
14
11
8
5
2
LII
LII+PAHs-LIF
PAHs-LIF
200
300
400
500
600
700
Emission wavelength λ em nm
Propane diffusion flame
Methane diffusion flame
DME diffusion flame